Theory and Practice of Science and Technology
2025, VOL. 6, NO. 8, 75-80
DOI: 10.47297/taposatWSP2633-456914.20250608

Experimental and Numerical Investigation on Film Cooling Characteristics of Fan-Shaped Holes under the Hot Streak Environment

Haozhe Yin

Shanghai Starriver Bilingual School, Shanghai, 201108, China

ABSTRACT

This study investigates the film cooling performance under hot streak conditions using both experimental measurements and numerical simulations. The analysis focuses on the variations in both the overall film cooling effectiveness and the adiabatic film cooling effectiveness on the surface of the thermal barrier coating (TBC) at different blowing ratios. The results indicate that the blowing ratio plays a critical role in enhancing both the momentum of the coolant jet and its attachment to the wall surface. However, excessively high jet momentum can lead to flow separation from the surface, thereby reducing the near-hole cooling performance. The evaluation of area-averaged film cooling effectiveness also reveals that cooling performance tends to plateau in the blowing ratio range of M = 2.0~3.0. In summary, film cooling performance under hot streak conditions demonstrates distinct characteristics, and the findings offer valuable insights for optimizing thermal protection strategies for high-temperature components.

KEYWORDS

Film cooling; Blowing ratio; Cooling effectiveness; Numerical simulation

1 Introduction

Gas turbines are critical power-generating devices in modern industrial systems, widely used in power generation, and propulsion. However, this field also faces multiple challenges, such as ensuring energy security and improve fuel economy [1]. Improving thermal efficiency is key to addressing these issues. The most effective way to enhance thermal efficiency is to increase the turbine inlet temperature (TIT), which, in turn, imposes stringent requirements on the thermal protection of hot-section components. Among these, turbine blades operate under the most severe thermal conditions. For instance, the inlet gas temperature can reach up to 1800 K, far exceeding the melting point of blade materials [2]. Prolonged exposure to such high temperatures significantly accelerates material degradation and can lead to structural failure, posing serious risks to turbine safety and service life. Thus, the development of advanced cooling technologies to protect turbine blades and extend their operational lifespan is of paramount importance.

Currently, several cooling strategies are employed for turbine blades, including TBC, Film Cooling [3], Effusive Cooling [4], and Internal Cooling. Among them, film cooling has been extensively studied due to its high efficiency and cost-effectiveness. Goldstein et al [5]. used multiple rows of thermocouples downstream of discrete holes to study the effects of hole geometry, secondary flow density, and mainstream boundary layer thickness on film cooling performance. Straub et al [6]. performed experimental measurements under conjugate heat transfer conditions using IR imaging to investigate the effect of downstream vortex generators. They found that vortex generators could improve lateral-averaged effectiveness by 1.5 times. Han et al [7]. used thermochromic liquid crystals to study flat-plate film cooling under various blowing ratios. Chen et al [8]. employed PSP to evaluate the influence of geometric parameters, blowing ratio, density ratio, and mainstream turbulence intensity. Extensive research has been conducted on the film cooling performance under different flow parameters and hole geometric parameters. These studies have significant engineering significance for predicting the film cooling performance and understanding the mechanism of film cooling.

Numerical simulations complement experiments by providing detailed physical insights that are otherwise difficult to obtain. Yang et al [9]. developed a conjugate heat transfer model of a blade cascade endwall and investigated the interaction between internal impingement and external film cooling. Koç et al [10]. numerically analyzed film cooling on curved and flat surfaces, showing that surface curvature alters near-wall flow structures and film coverage. Silieti et al [11]. compared adiabatic and conjugate models for fan-shaped holes, finding significant differences and highlighting the importance of metal conduction in temperature predictions. Zhao et al [12]. used LES to study pulsed film cooling with vortex generator pairs (VGPs), showing that VGPs created anti-counter-rotating vortex pairs (anti-CRVPs) that enhanced cooling.

During gas turbine operation, turbine blades not only endure steady high-temperature loads but also experience transient thermal shocks during startup, shutdown, or sudden load changes [9]. Additionally, the surface temperature is often non-uniform, leading to hot streaks caused by insufficient cooling coverage or uneven high-temperature flow. The migration of hot streaks through turbine stages can lead to local overheating and spalling of TBCs, thereby shortening blade life [13]. Moreover, these regions accelerate creep and thermal fatigue, increasing the risk of blade failure [14]. Barigozzi et al [15]. conducted experimental and numerical studies on hot streak migration in vane cascades with film cooling, using superposition principles to explain the interaction between mixing and coolant jets. However, studies focusing on fan-shaped holes under hot streak conditions are still limited. Therefore, the present study conducts both experimental and numerical investigations to explore the film cooling performance of fan-shaped holes under hot streak environments. The effects of various blowing ratios on cooling effectiveness and the underlying mechanisms are thoroughly analyzed.

2 Experimental investigation

2.1 Experimental setup

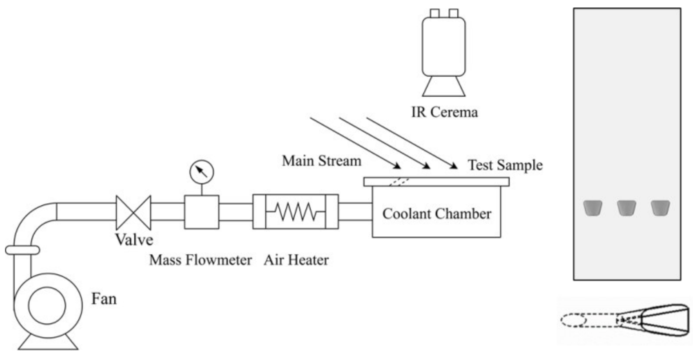

Figure 1 Schematic diagram of the experimental system and the test sample

The experimental setup is illustrated in Figure 1. The test article is subjected to a high-temperature mainstream flow that simulates the hot streak, with the mainstream temperature maintained at approximately 800 ℃. Cooling air is supplied by a blower and heated to 200 ℃ through a heat exchanger. The surface temperature of the test article is measured using IR camera. The schematic of the test article is also shown in Figure 1. The test sample is made of high-temperature alloy, and a ceramic coating is applied on the surface to simulate the thermal insulation behavior of TBCs. Fan-shaped film cooling holes are used, with an inclination angle of 30°, the hole diameter of $D = 5$mm and the length-to-diameter ratio of $L/D = 3$.

Once a stable film cooling layer is established and the surface temperature reaches a steady state, multiple thermal snapshots are captured using the infrared camera. These snapshots are then denoised and filtered to obtain the time-averaged surface temperature field. The surface temperature of the ceramic layer is nondimensionalized, and the TBC overall film cooling effectiveness is defined as:

$$\tau = \frac{T_m - T_s}{T_m - T_c}$$

where T_m is the average temperature of the mainstream, T_s is the temperature of the TBC surface, and T_c represents the temperature of the cooling air.

2.2 Experimental results and discussion

This experiment measured the temperature field on the surface of the TBC of a flat plate with a fan-shaped hole under different blowing ratios. Figure 2 shows the distribution of film cooling effectiveness on the TBC surface at different blowing ratios. The results indicate that, as the blowing ratio increases, the overall cooling effectiveness on the TBC

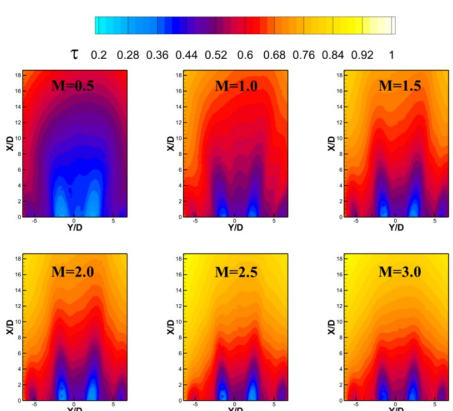

Figure 2 Overall film cooling effectiveness contour on the TBC surface at different blowing ratios

surface tends to increase. This trend can primarily be attributed to the increase in the coolant flow rate and momentum, enhancing the coolant's attachment and diffusion capabilities on the wall, thereby improving the local cooling performance. However, studies on cylindrical holes suggest that when the blowing ratio is too large, the high momentum of the coolant can intensify the shear interaction between the coolant and the high-temperature mainstream, which may induce jet detachment and flow separation from the wall, leading to local cooling failure [16]. Nevertheless, under the hot streak conditions in this study, no significant coolant detachment was observed downstream of the fan-shaped hole at any blowing ratio, and the overall cooling performance continued to improve with increasing blowing ratios.

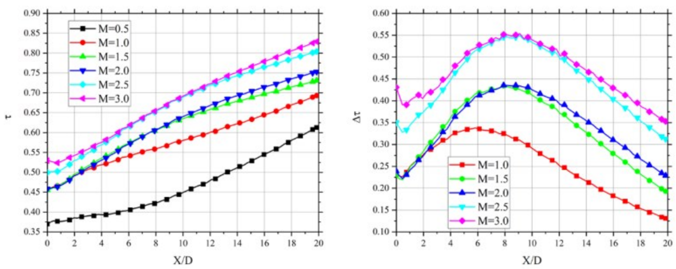

Figure 3 Centerline overall film cooling effectiveness and relative cooling effectiveness improvement rate on the TBC surface

The centerline overall film cooling effectiveness at different blowing ratios was calculated based on the temperature field on the TBC surface, as shown in Figure 3 (left). From the figure, it can be observed that the centerline cooling effectiveness is lowest at $M = 0.5$, and then monotonically increases with the blowing ratio, reaching the maximum value at $M = 3.0$. Additionally, at different blowing ratios, the centerline effectiveness also shows an increasing trend as the flow-wise normalized distance increases.

To quantify the enhancement of cooling capability at different blowing ratios, the relative improvement rate of the centerline film cooling effectiveness for each condition, with $M = 0.5$ as the baseline, was calculated, as shown in Figure 3 (right). The relative improvement rate is defined as:

$$\Delta\tau = \frac{\tau_{M=\mathrm{i}} - \tau_{M=0.5}}{\tau_{M=0.5}}$$

in which $i = 1.0$~3.0. The results indicate that the relative improvement rate generally increases with the blowing ratio, but exhibits a characteristic of first increasing and then decreasing along the flow direction. Meanwhile, the peak of the relative improvement rate shifts downstream with increasing blowing ratio. This suggests that the increased blowing ratio has a more significant effect on the middle section of the film cooling, which lies in the main mixing zone between the coolant and the high-temperature mainstream.

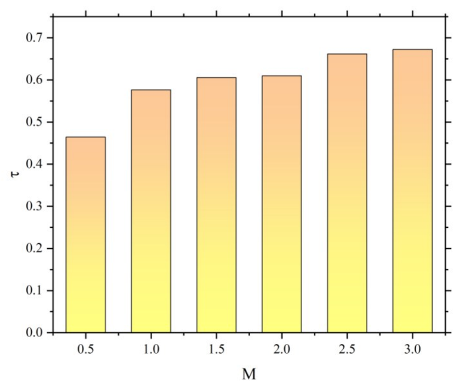

Figure 4 Area-averaged overall film cooling effectiveness on the TBC surface

Finally, the area-averaged cooling effectiveness on the TBC surface was calculated, as shown in Figure 4. The area-averaged cooling effectiveness on the TBC surface increases with the blowing ratio. The results indicate that the blowing ratio has a significant regulatory effect on the film cooling performance, but the improvement in cooling efficiency exhibits different characteristics along the flow direction. This is influenced by multiple factors, including jet-wall interaction, hot and cold stream mixing, and coolant dissipation.

3 Numerical investigation

3.1 Numerical method

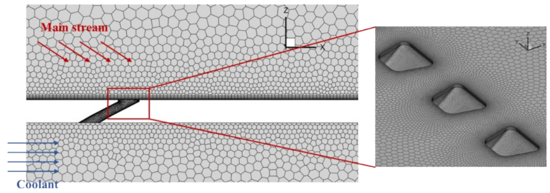

Figure 5 The computational domain and mesh

In this study, numerical simulations of the adiabatic film cooling performance under different blowing ratios were conducted using ANSYS Fluent. The flow was assumed to be compressible and steady-state, with no consideration of wall heat conduction, focusing solely on the film cooling efficiency under adiabatic conditions. The *SST k-ω* turbulence model was used, as it provides good performance in capturing near-wall flow and shear layer characteristics.

The computational domain was discretized using unstructured meshes generated by Fluent Meshing. The maximum dimensionless wall distance (y+) of approximately 1. The entire computational domain consists of approximately 4 million mesh cells, with mesh refinement based on mesh independence testing. The mesh independence verification is shown in Figure 6. When the number of mesh cells was increased to 4 million, the change in the area-averaged adiabatic film cooling effectiveness was less than 2% with further mesh refinement. The adiabatic film cooling effectiveness η is defined as:

$$\eta = \frac{T_m - T_{aw}}{T_m - T_c}$$

where T_{aw} is the adiabatic wall temperature. The boundary conditions are as follows: the mainstream is set as a velocity inlet with a velocity of 20 m/s, a temperature of 1073 K. The cooling air inlet is specified as a mass flow inlet with a temperature of 473 K. All outlets are set as pressure outlets. All walls are assumed to be adiabatic, no-slip walls.

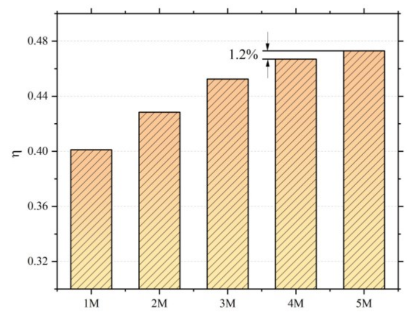

Figure 6 Mesh independence verification

3.2 Numerical results and discussion

The experimental results provide data for understanding the film cooling performance in a thermal stripe

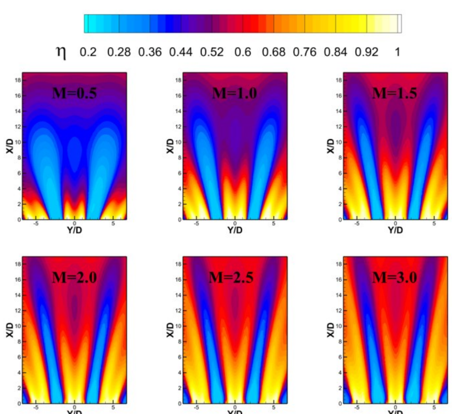

Figure 7 Adiabatic film cooling effectiveness contour under different blowing ratios

environment, but they are limited in revealing deeper mechanisms. This makes it possible for numerical simulations, which calculate the adiabatic film cooling effectiveness under the same boundary conditions, to serve as a supplement and explanation for the experimental results. Firstly, the adiabatic film cooling effectiveness contour maps under various operating conditions were compared, as shown in Figure 7. The cooling jet forms a distinct cooling agent streak downstream of the film hole, while a low cooling effectiveness streak forms between adjacent film holes. At the same time, the cooling agent streak exhibits a bimodal shape. The overall cooling efficiency increases with the blowing ratio, but the growth becomes slower in the high blowing ratio range ($M \geqslant 2.0$). At $M = 3.0$, the cooling streak near the film hole narrows due to the jet lift effect.

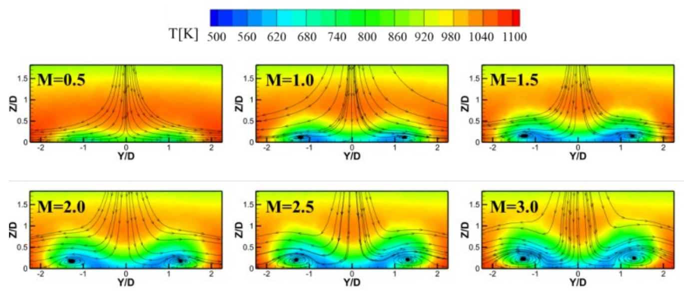

Figure 8 The temperature field and streamlines at the YZ cross-section downstream of the film hole for different blowing ratios

To further understand the physical mechanism behind this phenomenon, the temperature field and streamline distribution on the YZ plane at different blowing ratios were extracted, as shown in Figure 8. Downstream of the film hole, a distinct counter-rotating vortex pair (CVPs) is formed inside the cooling jet. As the blowing ratio increases, the size of the CVPs becomes larger, and the cooling jet extends further in the vertical wall direction. At the same time, with an increase in the blowing ratio, the CVPs tend to lift. The higher CVPs entrain the hot mainstream flow toward the underside of the cooling jet, thereby weakening the film cooling performance on the wall.

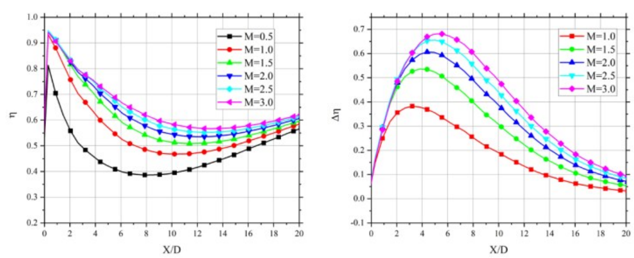

Figure 9 The centerline adiabatic film cooling effectiveness and relative cooling effectiveness enhancement rate downstream of the film hole

To further clarify the cooling performance along the centerline downstream of the film hole, the adiabatic cooling effectiveness and the relative cooling effectiveness enhancement rate curves along the centerline downstream of the film hole are plotted, as shown in Figure 9. The cooling effectiveness increases with the increase of the blowing ratio. The centerline efficiency curve shows a characteristic of first decreasing and then increasing. The position of the minimum cooling efficiency shifts further downstream from the film hole as the blowing ratio increases. The relative enhancement rate of cooling effectiveness shows a trend of first increasing and then decreasing.

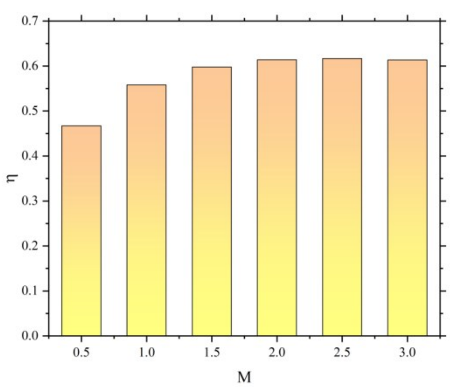

Figure 10 The area-averaged adiabatic film cooling effectiveness downstream of the film hole

To comprehensively quantify the overall cooling performance at different blowing ratios, the area-averaged adiabatic film cooling effectiveness in the downstream region of the film hole is compared, as shown in Figure 10. The results indicate that the area-averaged adiabatic film cooling effectiveness increases with the blowing ratio, with the most significant improvement observed in the range of M = 0.5 to 1.0. This suggests that increasing the coolant flow in the low blowing ratio range results in a significant cooling performance gain. Overall, film cooling relies on the cooling jet forming a thermal barrier layer on the wall, which blocks the direct heat exchange between the mainstream high-temperature gas and the wall, thereby reducing the wall temperature. However, when the blowing ratio is too high, the jet becomes difficult to adhere to the wall, forming a "film separation zone," which weakens the thermal insulation effect.

4 Conclusions

This paper focuses on the film cooling process under a thermal stripe environment, combining experimental studies and numerical simulations to investigate the variation of integrated film cooling effectiveness and adiabatic film cooling efficiency on the TBC surface at different blowing ratios. The main conclusions are as follows：

(1) The experimental results show that the cooling effectiveness on the TBC surface increases with the blowing ratio. The enhancement in cooling effectiveness shows different characteristics along the flow direction, which is influenced by the jet attachment to the wall, cold-hot mixing, and coolant dissipation.

(2) The numerical simulation results show that the adiabatic cooling efficiency increases with the blowing ratio. The adiabatic cooling efficiency is affected by the dissipation of the cooling jet along the flow direction and the uneven heat load in the thermal stripe environment。

(3) As the blowing ratio increases, the scale and height of CVPs increase. The uplift of CVPs weakens the film cooling performance. Additionally, the CVPs formed downstream of a fan-shaped hole extend laterally, enhancing the lateral spreading ability of the cooling jet.

(4) The film cooling process under a thermal stripe environment is more complex, and the cooling efficiency typically shows a nonlinear variation trend. Further research can focus on the multi-factor synergistic effect of different hole geometries and flow parameters to optimize the cooling performance under thermal stripe conditions.

References

[1] Advanced Technologies for Gas Turbines. Washington, D.C.: National Academies Press; 2020.
[2] Yang X, Liu Z, Zhao Q, Liu Z, Feng Z, Guo F, et al. Experimental and numerical investigations of overall cooling effectiveness on a vane endwall with jet impingement and film cooling. Applied Thermal Engineering 2019(148):1148–63.
[3] Bogard DG, Thole KA. Gas Turbine Film Cooling. Journal of Propulsion and Power 2006(22):249–70.
[4] Wang W, Yan Y, Zhou Y, Cui J. Review of Advanced Effusive Cooling for Gas Turbine Blades. Energies 2022;15:8568.
[5] Goldstein RJ, Eckert ERG, Burggraf F. Effects of hole geometry and density on three-dimensional film cooling. International Journal of Heat and Mass Transfer 1974;17:595–607.
[6] Straub D, Weber J, Roy A, Lee C-S, Shih TI-P. Effects of Downstream Vortex Generators on Film Cooling a Flat Plate Fed by Crossflow. Journal of Turbomachinery 2024;146:051011.
[7] Han Z, Liu S, Liu J, Zhou S, Liu J. Experimental Research on Film Cooling Characteristics at Different Blowing Ratios. Proceedings of the CSEE 2005:91–6.
[8] Chen AF, Li S-J, Han J-C. Film Cooling for Cylindrical and Fan-Shaped Holes Using Pressure-Sensitive Paint Measurement Technique. Journal of Thermophysics and Heat Transfer 2015;29:775–84.
[9] Yang X, Liu Z, Zhao Q, Liu Z, Feng Z, Guo F, et al. Experimental and numerical investigations of overall cooling effectiveness on a vane endwall with jet impingement and film cooling. Applied Thermal Engineering 2019;148:1148–63.
[10] Koç İ, Parmaksızogˇlu C, Çakan M. Numerical investigation of film cooling effectiveness on the curved surface. Energy Conversion and Management 2006;47:1231–46.
[11] Silieti M, Kassab AJ, Divo E. Film cooling effectiveness: Comparison of adiabatic and conjugate heat transfer CFD models. International Journal of Thermal Sciences 2009;48:2237–48.
[12] Zhao Z, Wen F, Tang X, Song J, Wang Z. Large eddy simulation of pulsed film cooling with vortex generators. International Journal of Heat and Mass Transfer 2021;180:121806.
[13] Swain B, Mallick P, Patel S, Roshan R, Mohapatra SS, Bhuyan S, et al. Failure analysis and materials development of gas turbine blades. Materials Today: Proceedings 2020;33:5143–6.
[14] Wang T, Xuan Y. Investigation of Unsteady Film Cooling Characteristics on the Hot Streak Migration Path. Journal of Engineering Thermophysics 2018;39:1991–6.
[15] Barigozzi G, Mosconi S, Perdichizzi A, Ravelli S. The Effect of Hot Streaks on a High Pressure Turbine Vane Cascade with Showerhead Film Cooling. IJTPP 2017;2:15.
[16] Goldstein RJ, Eckert ERG, Burggraf F. Effects of hole geometry and density on three-dimensional film cooling. International Journal of Heat and Mass Transfer 1974;17:595–607.